

Calculation of optical excitations in cubic semiconductors. III. Third-harmonic generation

W. Y. Ching and Ming-Zhu Huang

Department of Physics, University of Missouri-Kansas City, Kansas City, Missouri 64110

(Received 18 August 1992)

Following the preceding two papers on the linear optical and second-harmonic-generation calculations on the 18 cubic semiconductors of group-IV, III-V, and II-VI compounds using the first-principles band-structure method, the two nonzero elements $\chi_{111}^{(3)}(\omega)$ and $\chi_{1212}^{(3)}(\omega)$ of the third-order nonlinear susceptibility in these semiconductors are studied. Contributions to the third-harmonic generation from virtual-electron, virtual-hole, and three-state processes are investigated and the final results are compared with available experimental data. It is shown that the zero-frequency limits $\chi_{111}^{(3)}(0)$ and $\chi_{1212}^{(3)}(0)$ in these crystals can vary over several orders of magnitude, yet the ratios $\chi_{1212}^{(3)}(0)/\chi_{111}^{(3)}(0)$ show remarkable consistency and are in very good agreement with the available data. The frequency-dependent dispersion curves for the 18 semiconductors up to 10 eV are also calculated. For most crystals, structures are limited to the low-frequency range below 4.0 eV. For several crystals, $|\chi^{(3)}(\omega)|$ show additional resonance structures in the higher-frequency range that have never been revealed before. Correlations of $\chi^{(3)}(0)$ with direct band gap and $\chi^{(2)}(0)$ are investigated. There is a remarkable correlation between the direct gap and the triple of frequency of the leading peak in the dispersion curves. Our results are also compared with the other existing calculation by Moss, Ghahramani, Sipe, and van Driel on some of these crystals. We again emphasize the importance of having accurate conduction-band (CB) wave functions and in taking a sufficient number of CB states into the calculation in order to obtain converged results. This is far more important than other effects that are not taken into account in the present local-density calculation for the electronic states.

I. INTRODUCTION

In the preceding two papers^{1,2} (hereafter referred to as paper I and paper II), calculations of linear optical properties and the nonlinear second-harmonic generations (SHG) in cubic semiconductors using the first-principles band-structure method were described. This paper follows papers I and II and deals with the calculation of third-harmonic generations (THG) in the same crystals. THG is one of the simplest of all third-order nonlinear susceptibilities. Other third-order processes include three- or four-wave mixing, optical Kerr effect, optical bistability and phase conjugation, refractive index modulation, etc.³⁻⁷ Still, the THG process is extremely complicated even for the simplest crystals.⁴⁻⁷ Diagrammatic techniques have been used to describe various processes involving virtual states.⁷ The other simple third-order process that has been investigated is the resonant nonlinear refraction.⁸ While there are considerable experimental and theoretical works dealing with the third-order nonlinear optical process in large-gap insulators, ionic crystals, and rare-gas solids,⁹⁻¹⁵ there has been relatively little study of THG in cubic semiconductors. Like the SHG, most of the experimental measurements on THG in cubic semiconductors were done in the late 1960s or early 1970s. Although there has been an upsurge of interest in the enhancement of the high-order nonlinear optical process in semiconductor quantum wells, quantum dots, and superlattices in recent years,¹⁵⁻²¹ the fundamental process in the bulk semiconductor itself cannot be considered well understood.

Because of the general complexity of the third-order nonlinear optical processes, there were far fewer calculations for THG than for the SHG. Early theoretical calculation with THG in cubic semiconductors started with Jha and Bloembergen^{22,23} and Levine²⁴ in 1968, and were quickly followed by others.²⁵⁻²⁸ Wang²⁷ derived a simple empirical relation between hyperpolarizability [equivalent to $\chi^{(3)}(0)$] and linear polarizability [equivalent to $\chi^{(1)}(0)$]. Arya and Jha²⁹ used a simple sp^3 hybridization model with three parameters in the nearest-neighbor approximation to calculate $\chi^{(3)}(0)$ for C, Si, and Ge. Surprisingly good agreement with experiment was claimed with some of these calculations. Progress was limited with these model calculations because the empirical parameters used were never fully justified, and the lack of reliable data make critical comparison quite impossible. Following their earlier work on SHG,³⁰ Moss *et al.* (MGSV) presented a detailed scheme in 1990 (Ref. 31) to calculate the dispersion relation for $\chi_{111}^{(3)}(\omega)$ and $\chi_{1212}^{(3)}(\omega)$ using a full band-structure approach. Computationally efficient formulas were derived using the standard perturbation theory and the minimal-coupling interaction Hamiltonian. Different processes corresponding to virtual electron, virtual hole, and three states were clearly identified.³¹ Calculations of $|\chi_{111}^{(3)}(\omega)|$ and $|\chi_{1212}^{(3)}(\omega)|$ up to a photon frequency of 4 eV were performed for Si, Ge, and GaAs. Similar calculations were later extended to ZnSe, ZnTe, and CdTe.³² MGSV used two different methods for the electronic-structure calculation, the empirical-tight-binding (ETB) model,³³ and a minimal-basis, *semi-ab-initio* orthogonalized linear-

combination-of-atomic-orbitals (OLCAO) method of Huang and Ching.³⁴ Both methods gave $\chi^{(3)}(0)$ values that did not agree well with the measured data. However, the work of MGSV represents evaluation of the frequency-dependent dispersion relations of $\chi^{(3)}(\omega)$ for real semiconductor crystals.

In this paper, we present the results of our first-principles calculations of the frequency-dependent THG in the 18 cubic semiconductors. We follow the full band-structure approach of MGSV and neglect the effect of local-field corrections. We agree with MGSV that detailed electronic structure is a much more important factor in obtaining the correct values for THG than some other effects. Our work differs from MGSV in the following respects: (1) We use the first-principles self-consistent OLCAO method for the band-structures calculation as described in paper I, instead of the much less accurate tight-binding approximation or the *semi-ab-initio* OLCAO method;³⁴ (2) a scissor operator is applied to the conduction-band (CB) states to address the problem of gap underestimation associated with local-density approximations (LDA); (3) all the relevant momentum matrix elements (MME) are calculated with the Bloch functions throughout the entire Brillouin zone; (4) a sufficient number of high-CB states are included in the sum over states. This turns out to be a very important factor in obtaining accurate and converged results for THG as well as for the SHG;² (5) complete calculations are performed

for 18 semiconductors—three group-IV crystals (diamond, Si, and Ge), nine III-V compound semiconductors (AlP, AlAs, AlSb, GaP, GaAs, GaSb, InP, and InAs, InSb), and six II-VI semiconductor (ZnS, ZnSe, ZnTe, CdS, CdSe, and CdTe). We believe this to be the most comprehensive and detailed calculation of THG in bulk semiconductors to date.

In Sec. II, we outline the specific procedures for the calculation of THG using the band-structure approach. In Sec. III, we present and discuss the central result of the paper, the calculation of THG for 18 semiconductors. The paper ends with a brief conclusion in the last section.

II. METHOD AND APPROACH

In order to make this paper self-contained, we will outline the method of our calculation even though it follows closely from MGSV (Ref. 31) and is parallel to the calculation of $\chi^{(2)}(\omega)$ in paper II. According to MGSV, the imaginary part of the complex $\chi^{(3)}(\omega)$ function consists of three contributions corresponding to the virtual-electron (VE), virtual-hole (VH), and three-state (3S) processes. The VH process consists of three different types, VH1, VH2, and VH3. The specific formulas for crystals with cubic symmetry suitable for computation are listed below after the apparent divergent terms are discarded on physical grounds.³¹

$$\text{Im}[\chi_{\text{VE}}^{(3)}(\omega)] = -\frac{\pi}{3} \left[\frac{e\hbar}{m} \right]^4 \int_{\text{BZ}} \frac{d\mathbf{k}}{4\pi^3} \sum_{ijkl} \text{Re}[P_{ij}^{vc} P_{jk}^{cc} P_{kl}^{cc} P_{li}^{cv}] \left[\mathcal{A}1 \frac{\delta(E_{ji} - 3\hbar\omega)}{E_{ji}^4} + \mathcal{A}2 \frac{\delta(E_{ki} - 2\hbar\omega)}{E_{ki}^4} + \mathcal{A}3 \frac{\delta(E_{li} - \hbar\omega)}{E_{li}^4} \right], \quad (1)$$

$$\text{Im}[\chi_{\text{VH1}}^{(3)}(\omega)] = -\frac{\pi}{3} \left[\frac{e\hbar}{m} \right]^4 \int_{\text{BZ}} \frac{d\mathbf{k}}{4\pi^3} \sum_{ijkl} \text{Re}[P_{ij}^{vc} P_{li}^{vv} P_{kl}^{vv} P_{jk}^{cv}] \left[\mathcal{B}1 \frac{\delta(E_{ji} - 3\hbar\omega)}{E_{ji}^4} + \mathcal{B}2 \frac{\delta(E_{jl} - 2\hbar\omega)}{E_{jl}^4} + \mathcal{B}3 \frac{\delta(E_{jk} - \hbar\omega)}{E_{jk}^4} \right], \quad (2a)$$

$$\text{Im}[\chi_{\text{VH2}}^{(3)}(\omega)] = +\frac{\pi}{3} \left[\frac{e\hbar}{m} \right]^4 \int_{\text{BZ}} \frac{d\mathbf{k}}{4\pi^3} \sum_{ijkl} \text{Re}[P_{ij}^{vc} P_{jk}^{cc} P_{li}^{vv} P_{kl}^{cv}] \left[\mathcal{C}1 \frac{\delta(E_{ji} - 3\hbar\omega)}{E_{ji}^4} + \mathcal{C}2 \frac{\delta(E_{ki} - 2\hbar\omega)}{E_{ki}^4} + \mathcal{C}3 \frac{\delta(E_{kl} - \hbar\omega)}{E_{kl}^4} \right], \quad (2b)$$

$$\text{Im}[\chi_{\text{VH3}}^{(3)}(\omega)] = +\frac{\pi}{3} \left[\frac{e\hbar}{m} \right]^4 \int_{\text{BZ}} \frac{d\mathbf{k}}{4\pi^3} \sum_{ijkl} \text{Re}[P_{ij}^{vc} P_{li}^{vv} P_{jk}^{cc} P_{kl}^{cv}] \left[\mathcal{D}1 \frac{\delta(E_{ji} - 3\hbar\omega)}{E_{ji}^4} + \mathcal{D}2 \frac{\delta(E_{jl} - 2\hbar\omega)}{E_{jl}^4} + \mathcal{D}3 \frac{\delta(E_{kl} - \hbar\omega)}{E_{kl}^4} \right], \quad (2c)$$

$$\text{Im}[\chi_{\text{3S}}^{(3)}(\omega)] = +\frac{\pi}{3} \left[\frac{e\hbar}{m} \right]^4 \int_{\text{BZ}} \frac{d\mathbf{k}}{4\pi^3} \sum_{ijkl} \text{Re}[P_{ij}^{vc} P_{jk}^{cv} P_{kl}^{vc} P_{li}^{cv}] \left[\mathcal{E}1 \frac{\delta(E_{ji} - 3\hbar\omega)}{E_{ji}^4} + \mathcal{E}2 \frac{\delta(E_{li} - \hbar\omega)}{E_{li}^4} \right], \quad (3)$$

where

$$\begin{aligned} \mathcal{A}1 &= \frac{729}{(3E_{ki} - 2E_{ji})(3E_{li} - E_{ji})}, \quad \mathcal{A}2 = \frac{128(2E_{ji} - E_{ki})}{(2E_{li} - E_{ki})(2E_{ji} - 3E_{ki})(2E_{ji} + E_{ki})}, \\ \mathcal{A}3 &= \frac{1}{(E_{ki} - 2E_{li})} \left[\frac{1}{(E_{ji} - 3E_{li})} + \frac{2E_{ki}}{(E_{li} + E_{ji})(E_{ki} + 2E_{li})} \right], \\ \mathcal{B}1 &= \frac{729}{(3E_{jl} - 2E_{ji})(3E_{jk} - E_{ji})}, \quad \mathcal{B}2 = \frac{128(2E_{ji} - E_{jl})}{(2E_{jk} - E_{jl})(2E_{ji} - 3E_{jl})(2E_{ji} + E_{jl})}, \end{aligned}$$

$$\begin{aligned}
\mathcal{B}3 &= \frac{1}{(E_{jl} - 2E_{jk})} \left[\frac{1}{(E_{ji} - 3E_{jk})} + \frac{2E_{jl}}{(E_{jk} + E_{ji})(E_{jl} + 2E_{jk})} \right], \\
\mathcal{C}1 &= \frac{729}{(3E_{ki} - 2E_{ji})(3E_{kl} - E_{ji})}, \quad \mathcal{C}2 = \frac{128(2E_{ji} - E_{ki})}{(2E_{kl} - E_{ki})(2E_{ji} - 3E_{ki})(2E_{ji} + E_{ki})}, \\
\mathcal{C}3 &= \frac{1}{(E_{ki} - 2E_{kl})} \left[\frac{1}{(E_{ji} - 3E_{kl})} + \frac{2E_{ki}}{(E_{kl} + E_{ji})(E_{ki} + 2E_{kl})} \right], \\
\mathcal{D}1 &= \frac{729}{(3E_{jl} - 2E_{ji})(3E_{kl} - E_{ji})}, \quad \mathcal{D}2 = \frac{128(2E_{ji} - E_{jl})}{(2E_{kl} - E_{jl})(2E_{ji} - 3E_{jl})(2E_{ji} + E_{jl})}, \\
\mathcal{D}3 &= \frac{1}{(E_{jl} - 2E_{kl})} \left[\frac{1}{(E_{ji} - 3E_{kl})} + \frac{2E_{jl}}{(E_{kl} + E_{ji})(E_{jl} + 2E_{kl})} \right], \\
\mathcal{E}1 &= \frac{729}{(3E_{jk} - E_{ji})(3E_{li} - E_{ji})}, \\
\mathcal{E}2 &= \frac{1}{(E_{jk} + 3E_{li})} \left[\frac{(E_{lk} + E_{jk})}{(E_{lk} - 3E_{li})(E_{ji} + E_{li})} + \frac{(E_{ji} + E_{jk})}{(E_{ji} - 3E_{li})(E_{lk} + E_{li})} \right].
\end{aligned}$$

Here, i, j, k , and l are the band indices, v and c indicate whether the state is in valence band (VB) or in conduction band, and $E_{ij} = E_i - E_j$, $P_{ij} = -i\hbar \langle i | \nabla | j \rangle$ is the MME. In the VE and VH processes, four states are involved. For the VE process, one state is in the VB and three in the CB, and the MME product contains two CB-CB matrix elements. The VH process consists of three types,³¹ one with three states in the VB and one in the CB, the other two types with two states each in the VB and the CB. Only the last two types contain the CB-CB matrix in the MME product. In the 3S term, only three states are involved, one in the VB and two in the CB and the MME product contains no CB-CB matrix element. This 3S contribution in $\chi^{(3)}(\omega)$ is different from the SHG calculation of paper II, in which the MME product contains a CB-CB matrix element in a three-state transition. As will be discussed later, all three types of processes can make significant contributions and should not be neglected. The VE and VH processes make negative contributions, yet the overall sign of $\chi^{(3)}(0)$ is positive because the 3S is dominating and positive. It is clear from Eqs. (1), (2), and (3) that each type of contribution consists of an ω term, a 2ω term, and a 3ω term. It is the 3ω term that is more directly linked to the THG and is expected to dominate in the low-frequency region. The resonance δ functions in Eqs. (1)–(3) are evaluated using an energy window of 0.01 eV, which is determined by detailed testing so as to be consistent with the number of \mathbf{k} points used in the sum over the Brillouin zone (BZ). We have used 505 \mathbf{k} points with appropriate weighting factors in the $\frac{1}{48}$ of the BZ to evaluate the sum over BZ. This number of \mathbf{k} -point sampling gives us an accuracy of about 5% with respect to the k -space convergence. This level of \mathbf{k} -point sampling is found to be reasonably adequate without succumbing to excessive computational demand. One may be able to improve the \mathbf{k} -space convergence by employing some kind of interpolation scheme but we decided to use only the \mathbf{k} points where the energy eigenvalues and the MME are calculated *ab initio*.

As was discussed in Sec. I of paper II, there are only two independent nonzero elements $\chi_{1111}^{(3)}(\omega)$ and $\chi_{1212}^{(3)}(\omega)$ for THG in crystals with cubic symmetry. The computation of these specific elements entails the appropriate choice of the components of the MME in the numerator of Eqs. (1), (2), and (3). In a completely isotropic material, $\chi_{1111}^{(3)}(\omega) = 3\chi_{1212}^{(3)}(\omega)$. In the present study, both elements are calculated so that the degree of anisotropy in THG in the cubic semiconductors can be checked. It is advantageous to calculate the energy denominator in Eqs. (1)–(3) and the MME products separately, since the former only need to be evaluated once for both elements.

The real part of $\chi^{(3)}(\omega)$ is obtained from the imaginary part by Kramers-Kronig (KK) conversion. The validity of using KK conversion to calculate THG can be checked by comparing the zero-frequency values of $\text{Re}[\chi_{1111}^{(3)}(0)]$ and $\text{Re}[\chi_{1212}^{(3)}(0)]$ with the same values calculated independently using the formulas before the resonance expansion that gives rise to the δ functions and by setting $\omega = 0$. These are given by

$$\begin{aligned}
\chi_{\text{VE}}^{(3)}(0) &= -\frac{2}{3} \left[\frac{e\hbar}{m} \right]^4 \\
&\times \int_{\text{BZ}} \frac{d\mathbf{k}}{4\pi^3} \sum_{ijkl} \text{Re}[P_{ij}^{vc} P_{jk}^{cc} P_{kl}^{cc} P_{li}^{cv}] \\
&\times \left[\frac{\mathcal{A}1}{E_{ji}^5} + \frac{\mathcal{A}2}{E_{ki}^5} + \frac{\mathcal{A}3}{E_{li}^5} \right], \quad (4)
\end{aligned}$$

$$\begin{aligned}
\chi_{\text{VH1}}^{(3)}(0) &= -\frac{2}{3} \left[\frac{e\hbar}{m} \right]^4 \\
&\times \int_{\text{BZ}} \frac{d\mathbf{k}}{4\pi^3} \sum_{ijkl} \text{Re}[P_{ij}^{vc} P_{li}^{vv} P_{kl}^{vv} P_{jk}^{cv}] \\
&\times \left[\frac{\mathcal{B}1}{E_{ji}^5} + \frac{\mathcal{B}2}{E_{jl}^5} + \frac{\mathcal{B}3}{E_{jk}^5} \right], \quad (5a)
\end{aligned}$$

$$\chi_{\text{VH2}}^{(3)}(0) = + \frac{2}{3} \left[\frac{e\hbar}{m} \right]^4 \times \int_{\text{BZ}} \frac{d\mathbf{k}}{4\pi^3} \sum_{ijkl} \text{Re}[P_{ij}^{vc} P_{jk}^{cc} P_{li}^{vv} P_{kl}^{cv}] \times \left[\frac{\mathcal{C}1}{E_{ji}^5} + \frac{\mathcal{C}2}{E_{ki}^5} + \frac{\mathcal{C}3}{E_{kl}^5} \right], \quad (5b)$$

$$\chi_{\text{VH3}}^{(3)}(0) = + \frac{2}{3} \left[\frac{e\hbar}{m} \right]^4 \times \int_{\text{BZ}} \frac{d\mathbf{k}}{4\pi^3} \sum_{ijkl} \text{Re}[P_{ij}^{vc} P_{li}^{vv} P_{jk}^{cc} P_{kl}^{cv}] \times \left[\frac{\mathcal{D}1}{E_{ji}^5} + \frac{\mathcal{D}2}{E_{jl}^5} + \frac{\mathcal{D}3}{E_{kl}^5} \right], \quad (5c)$$

$$\chi_{\text{3S}}^{(3)}(0) = + \frac{2}{3} \left[\frac{e\hbar}{m} \right]^4 \int_{\text{BZ}} \frac{d\mathbf{k}}{4\pi^3} \sum_{ijkl} \text{Re}[P_{ij}^{vc} P_{jk}^{cv} P_{kl}^{vc} P_{li}^{cv}] \times \left[\frac{\mathcal{E}1}{E_{ji}^5} + \frac{\mathcal{E}2}{E_{li}^5} \right]. \quad (6)$$

Calculation for $\chi^{(3)}(0)$ according to the above equations is considered to be more direct and therefore more accurate. We find the agreement between the two ways of calculating $\chi^{(3)}(0)$ to be within 5–10 % for most crystals.

In paper II, we have stressed the importance of taking a sufficient number of accurately determined CB states into the sum over states. This is equally true for the THG calculation. Because the energy dependence in $\chi^{(3)}(\omega)$ is now $1/E^7$, as opposed to $1/E^5$ in $\chi^{(2)}(\omega)$, and

also because the dominating contribution to $\chi^{(3)}(\omega)$ is from the 3S term that does not contain any CB-CB MME; the CB cutoff energy needed for a converged result in $\chi^{(3)}(\omega)$ is somewhat less stringent than those for $\chi^{(2)}(\omega)$. However, the demand for the accuracy of the wave function is actually increased because the VE term of Eq. (1) involves products of two CB-CB MME instead of one in $\chi^{(2)}(\omega)$. Since the calculation of $\chi^{(3)}(\omega)$ is much more time consuming than $\chi^{(2)}(\omega)$, the CB cutoff energy adopted in the $\chi^{(3)}(\omega)$ calculation is determined by the overall consideration of convergency, accuracy, and efficiency. The CB cutoff energy E_{cf} used in the present calculation for $\chi^{(3)}(\omega)$ for the 18 semiconductors are listed in Table I. They are about 10 eV less than that for $\chi^{(2)}(\omega)$ in paper II.

III. RESULTS OF CALCULATION

In this section, we present the results of our calculation for the THG in 18 semiconductors. We divide them into three groups, the group-IV elements diamond, Si, and Ge; the III-V compounds Al, Ga, and In series; and the II-VI compounds of the Zn and Cd series. Tables I and II present the calculated values for $\chi_{1111}^{(3)}(0)$ and $\chi_{1212}^{(3)}(0)$ which are broken into three separate contributions from the VE, VH, and 3S parts. Also listed are the cutoff energy used for each crystal. For all the semiconductors studied, the contributions from VE and VH to $\chi_{1111}^{(3)}(0)$ are negative and that from the 3S term is positive and overwhelming, thus resulting in the overall positive values for $\chi_{1111}^{(3)}(0)$. For $\chi_{1212}^{(3)}(0)$, they are some positive but negligible VE contributions from a few crystals. Taking GaAs as an example, the contribution to $\chi_{1111}^{(3)}(0)$ from the VE, VH, and 3S contributions are -7.64 , -2.28 , and 16.87 (in units of 10^{-11} esu), respectively.

TABLE I. Cutoff frequency and virtual-electron, virtual-hole, and three-state contributions to $\chi_{1111}^{(3)}(0)$ (in units of 10^{-11} esu).

| Crystal | E_{cf} (eV) | Virtual electron | Virtual hole | Three state | Total | by KK |
|---------|----------------------|------------------|--------------|-------------|---------|---------|
| C | 15 | -0.008 | -0.001 | 0.066 | 0.057 | 0.058 |
| Si | 20 | -0.56 | -0.34 | 3.97 | 3.07 | 3.62 |
| Ge | 15 | -11.33 | -4.93 | 46.95 | 30.69 | 33.98 |
| AlP | 30 | -0.32 | -0.21 | 1.92 | 1.39 | 1.34 |
| AlAs | 15 | -0.80 | -0.25 | 2.02 | 0.97 | 0.99 |
| AlSb | 35 | -9.15 | -1.55 | 18.22 | 7.52 | 7.38 |
| GaP | 15 | -1.01 | -0.37 | 3.48 | 2.10 | 2.00 |
| GaAs | 25 | -7.64 | -2.28 | 16.87 | 6.95 | 6.77 |
| GaSb | 30 | -40.86 | -19.94 | 248.0 | 187.2 | 204.6 |
| InP | 20 | -9.98 | -3.16 | 22.98 | 9.84 | 8.28 |
| InAs | 30 | -157 | -192 | 10 528 | 10 179 | 8 956 |
| InSb | 30 | -933 | -1989 | 419 825 | 417 836 | 350 070 |
| ZnS | 15 | -0.09 | -0.044 | 0.333 | 0.20 | 0.25 |
| ZnSe | 20 | -0.19 | -0.12 | 0.86 | 0.55 | 0.58 |
| ZnTe | 26 | -0.72 | -0.54 | 4.14 | 2.87 | 2.77 |
| CdS | 15 | -0.35 | -0.18 | 1.53 | 1.00 | 0.87 |
| CdSe | 25 | -1.40 | -0.68 | 5.03 | 2.95 | 3.17 |
| CdTe | 15 | -5.45 | -1.49 | 12.35 | 5.41 | 5.72 |

TABLE II. Cutoff frequency and virtual-electron, virtual-hole, and three-state contributions to $\chi_{1212}^{(3)}(0)$ (in units of 10^{-11} esu).

| Crystal | E_{cf} (eV) | Virtual electron | Virtual hole | Three state | Total | by (KK) |
|---------|---------------|------------------|--------------|-------------|--------|---------|
| C | 15 | -0.0004 | -0.001 | 0.033 | 0.031 | 0.042 |
| Si | 20 | -0.10 | -0.23 | 2.23 | 1.90 | 2.19 |
| Ge | 15 | -1.07 | -4.03 | 15.37 | 10.27 | 10.41 |
| AlP | 30 | -0.03 | -0.14 | 1.10 | 0.92 | 0.90 |
| AlAs | 15 | -0.08 | -0.15 | 0.96 | 0.73 | 0.73 |
| AlSb | 35 | -3.46 | -1.30 | 10.32 | 5.54 | 5.52 |
| GaP | 15 | 0.006 | -0.30 | 1.62 | 1.34 | 1.42 |
| GaAs | 25 | -1.17 | -1.86 | 7.05 | 4.01 | 4.16 |
| GaSb | 30 | -2.08 | -17.10 | 61.87 | 42.7 | 41.3 |
| InP | 20 | -1.68 | -2.70 | 10.07 | 5.69 | 4.13 |
| InAs | 30 | 41 | -169 | 1094 | 966 | 1006 |
| InSb | 30 | 62 | -592 | 15 248 | 14 718 | 12 574 |
| ZnS | 15 | 0.009 | -0.031 | 0.169 | 0.15 | 0.16 |
| ZnSe | 20 | 0.015 | -0.105 | 0.42 | 0.33 | 0.34 |
| ZnTe | 26 | -0.04 | -0.45 | 2.02 | 1.53 | 1.65 |
| CdS | 15 | 0.05 | -0.157 | 0.68 | 0.57 | 0.60 |
| CdSe | 25 | 0.11 | -0.59 | 2.00 | 1.52 | 1.60 |
| CdTe | 15 | -0.68 | -1.36 | 6.06 | 4.02 | 4.67 |

The same numbers for $\chi_{1212}^{(3)}(0)$ for GaAs are -1.17, -1.86, and 7.05, respectively. Also listed in the last column of Tables I and II are the results for $\chi_{1111}^{(3)}(0)$ and $\chi_{1212}^{(3)}(0)$, obtained from the real part of $\chi^{(3)}(\omega)$ through KK conversion. The agreements with those obtained directly from Eqs. (4)–(6) are generally within 10%. This gives us confidence in the calculated dispersion relations $\chi_{1111}^{(3)}(\omega)$ and $\chi_{1212}^{(3)}(\omega)$ that will be discussed later.

In Table III, we compare our calculated results of $\chi_{1111}^{(3)}(0)$ and $\chi_{1212}^{(3)}(0)$ with experimental data^{35–44} and other existing calculations.^{22,24–26,28,29,31,32} The experimental data may contain large error bars and in some cases there is the problem of an extra factor of 4 because of the different ways of defining the third-order susceptibility tensor. Original references should be consulted for details. Measured data are available only for C, Si, Ge, GaAs, and InSb. It is gratifying that our calculated results are in very good agreement with the data for all these crystals, realizing that experimental uncertainty renders any results beyond the order of magnitude established in the data quite meaningless. For InSb, the measured $\chi_{1111}^{(3)}(0)$ values are extremely large, presumably due to the very small direct band gap in InSb. The three data from Refs. 40, 43, and 44 differ by four orders of magnitude. Our calculated value lies somewhere between these experimental large values. For CdS, we cannot locate any reliable data for bulk crystal to compare. Cheng, Herron, and Wang⁴⁵ measured the THG in a series of small CdS clusters (< 30 Å) and found $\chi^{(3)}(0)$ to vary from 0.5 to 33 (in units of 10^{-11} esu) at 1.9 μm . Since quantum dots of appropriate size are supposed to enhance optical nonlinearity, these measured values are certainly consistent with our calculated bulk value of $\chi_{1111}^{(3)}(0) = 1.0 \times 10^{-11}$ esu and $\chi_{1212}^{(3)}(0) = 0.57 \times 10^{-11}$ esu. It is highly desirable that measurements on these crystals be repeated.

The ratio $\chi_{1212}^{(3)}(0)/\chi_{1111}^{(3)}(0)$ should be a more reliable

indicator of the accuracy of calculation since systematic error in the experimental measurements may be canceled out. For a completely isotropic medium, this ratio will be $\frac{1}{3}$. Our calculation shows that only Ge has a ratio close to $\frac{1}{3}$. For most crystals, the isotropic ratio lies in the range of 0.5–0.75, with the small-gap semiconductors (GaSb, InAs, and InSb) as exceptions. For a few crystals where both $\chi_{1111}^{(3)}(0)$ and $\chi_{1212}^{(3)}(0)$ data are available, the agreement with our calculation in this isotropic ratio is quite good, especially for GaAs.

Also listed in Table III are the calculations done by some other groups. Arya and Jha²⁹ had calculated $\chi_{1111}^{(3)}(0)$ using a tight-binding Hamiltonian in which the parameters were fixed by fitting to known experimental values for the VB width, direct band gap, and the linear dielectric constant. Good agreement for C was obtained but the results for Si and Ge were greatly underestimated. While some of these calculations show good agreement with data for some crystals, the empirical nature of these calculations makes it difficult to assess their validity. For example, the model calculation by Flytzanis²⁶ gave reasonably good agreement for Ge and GaAs, but failed miserably on InSb. We shall compare our results more directly with the calculations done by MGSV using the full-band-structure approach.³¹ MGSV calculated both $\chi_{1111}^{(3)}(0)$ and $\chi_{1212}^{(3)}(0)$ for Si, Ge, and GaAs. They used the ETB method and also a more rigorous *semi-ab-initio* band method, and found the former to give results in better agreement with experiments. It is clear to us that the severe underestimation by MGSV using the *semi-ab-initio* method is actually due to the insufficient number of CB band states in the sum over states. The result of using the ETB approximation is likely to be misleading since the closer agreement with experiment is the consequence of the rather arbitrary ways of estimating the MME. When Ghahramani, Moss, and Sipe (GMS) later extended the calculation to the three II-VI compounds

ZnSe, ZnTe, and CdTe using the same *semi-ab-initio* method,³² their results were again more than an order of magnitude smaller than our first-principles results in which sufficient CB states are included to ensure convergence.

Some other general observations of the results listed in Table III are (1) within each series, the $\chi^{(3)}(0)$ increases as the atomic number of the second element increases; (2) the II-VI compounds have smaller values of $\chi^{(3)}(0)$ than the III-V compounds; (3) there are large variations in $\chi^{(3)}(0)$ values ranging from the smallest of 0.057×10^{-11} esu in C to the largest of $417\,800 \times 10^{-11}$ esu in InSb.

We now discuss the frequency-dependent dispersion re-

lations in $\chi^{(3)}(\omega)$ for each crystal. Since there is no available experimental data to compare, we consider our results of $\chi^{(3)}(\omega)$ to be theoretical predictions waiting for experimental confirmation.

A. Group-IV elements

The calculated dispersion relations for $\chi_{1111}^{(3)}(\omega)$ and $\chi_{1212}^{(3)}(\omega)$ for C, Si, and Ge are shown in Figs. 1, 2, and 3, respectively. The upper panel shows the real and imaginary parts for $\chi_{1111}^{(3)}(\omega)$ and the middle panel shows the real and imaginary parts for $\chi_{1212}^{(3)}(\omega)$. The lower panel

TABLE III. Calculated third-harmonic generation in cubic semiconductors.

| Crystal | $\chi_{1111}^{(3)}(0)$ (10^{-11} esu) | | | $\chi_{1212}^{(3)}(0)$ (10^{-11} esu) | | | $\chi_{1212}^{(3)}(0)/\chi_{1111}^{(3)}(0)$ | |
|---------|--|---------------------|--------------------|--|--------------------|--------------------|---|-------|
| | Present calc. | Expt. | Other calc. | Present calc. | Expt. | Other calc. | Present calc. | Expt. |
| C | 0.057 | 0.0184 ^a | 0.017 ^b | 0.031 | 0.007 ^a | | 0.55 | 0.26 |
| Si | 3.07 | 2.4 ^c | 26 ^d | 1.90 | 1.15 ^c | | 0.62 | 0.48 |
| | | 33 ^e | 1.75 ^f | | | 1.24 ^f | 0.53 | |
| | | 20 ^g | 3.6 ^h | | | 2.6 ^h | | |
| | | | 0.8 ⁱ | | | 0.5 ⁱ | | |
| Ge | 30.69 | | 4.8 ^j | 10.27 | 24 ^c | 2.3 ^j | 0.33 | 0.60 |
| | | 40 ^c | 64 ^d | | | | | |
| | | 10 ^k | 12 ^f | | | 9.6 ^f | | |
| | | 16 ^l | 16 ^h | | | 12 ^h | | |
| | | 12 ^e | 2.7 ^b | | | | | |
| | | 4.1 ^g | 6.9 ⁱ | | | 6.9 ⁱ | | |
| AlP | 1.39 | | 206 ^j | 0.92 | | 102 ^j | 0.66 | |
| | | | | | | | | |
| | | | | | | | | |
| | | | | | | | | |
| | | | | | | | | |
| | | | | | | | | |
| | | | | | | | | |
| | | | | | | | | |
| | | | | | | | | |
| | | | | | | | | |
| AlAs | 3.97 | | | 0.73 | | | 0.75 | |
| AlSb | 7.52 | | 0.9 ^f | 5.54 | | 0.5 ^f | 0.74 | |
| GaP | 2.10 | | 1.0 ^f | 1.34 | | 0.5 ^f | 0.64 | |
| GaAs | 6.95 | 3.9 ^m | 3.12 ⁿ | 4.01 | 2.0 ^m | 2.03 ⁿ | 0.58 | 0.53 |
| | | 4.8 ^c | 2.4 ^f | | | 1.2 ^f | | |
| | | 18 ^e | 3.8 ^h | | | 2.8 ^h | | |
| | | | 0.7 ⁱ | | | 0.77 ⁱ | | |
| | | | 8.0 ^j | | | 4.7 ^j | | |
| GaSb | 187.2 | | 7.4 ^f | 42.7 | | 5.1 ^f | 0.23 | |
| InP | 9.84 | | 3.0 ^f | 5.69 | | 1.5 ^f | 0.58 | |
| InAs | 10 179 | | 6.2 ^f | 966 | | 3.0 ^f | 0.10 | |
| InSb | 417 836 | 10 ^{9o} | 1.51 ^f | 14 718 | | 0.79 ^f | 0.034 | |
| | | 8000 ^p | | | | | | |
| | | 10 ^{11q} | | | | | | |
| ZnS | 0.20 | | | 0.15 | | | 0.75 | |
| ZnSe | 0.55 | | 0.02 ^r | 0.33 | | 0.037 ^r | 0.60 | |
| ZnTe | 2.87 | | 0.06 ^r | 1.53 | | 0.073 ^r | 0.53 | |
| CdS | 1.00 | | 0.25 ^d | 0.57 | | | 0.57 | |
| CdSe | 2.95 | | | 1.52 | | | 0.52 | |
| CdTe | 5.41 | | 0.03 ^r | 4.02 | | 0.22 ^r | 0.74 | |

^aReference 39.

^bReference 21.

^cReference 15.

^dReference 17.

^eReference 36.

^fReference 19.

^gReference 37.

^hReference 20.

ⁱReference 23, using the *semi-ab-initio* method.

^jReference 23, using the ETB method.

^kReference 41.

^lReference 42.

^mReference 38.

ⁿReference 18.

^oReference 40.

^pReference 44.

^qReference 43.

^rReference 24, using the *semi-ab-initio* method.

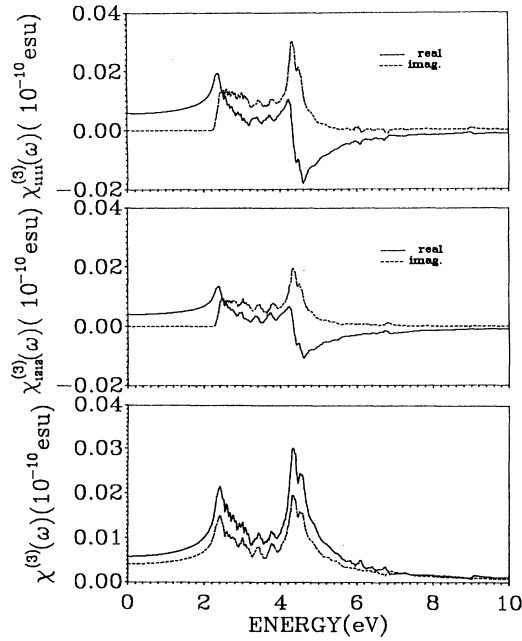


FIG. 1. Calculated third-harmonic generations for C. (a) $\chi_{1111}^{(3)}(\omega)$, real part, solid line; imaginary part, dashed line. (b) $\chi_{1212}^{(3)}(\omega)$, real part, solid line; imaginary part, dashed line. (c) Solid line: $|\chi_{1111}^{(3)}(\omega)|$; dashed line: $|\chi_{1212}^{(3)}(\omega)|$.

shows $|\chi_{1111}^{(3)}(\omega)|$ and $|\chi_{1212}^{(3)}(\omega)|$. (From here on, the dispersion curves for all the semiconductors studied are presented in this fashion.) We shall concentrate our discussion on the lower panel, and on $|\chi_{1111}^{(3)}(\omega)|$ in particular, since $|\chi_{1212}^{(3)}(\omega)|$ is more or less parallel to $|\chi_{1111}^{(3)}(\omega)|$ except in the high-frequency region where resonance peaks may appear. Figures 1–3 show that C has a double peak, Si has a triple peak, and Ge has multiple peaks. The leading peaks in these three crystals are at 2.4, 1.3, and 0.4 eV, respectively. (We shall arbitrarily label those peaks above 3 eV as resonance peaks except for C.) Ge also has a very strong resonance peak at 4.7 eV. The positions of the major peaks in $|\chi_{1111}^{(3)}(\omega)|$ are listed in Table IV. Minor peaks are not listed and inspection of the dispersion curves should be the best way to provide the most detailed information.

B. III-V semiconductors

The dispersion curves for $\chi_{1111}^{(3)}(\omega)$ and $\chi_{1212}^{(3)}(\omega)$ for AlP, AlAs, and AlSb are shown in Figs. 4, 5, and 6, respectively. For AlP, $|\chi^{(3)}(\omega)|$ consists of a broad peak centered at 1.7 eV with no resonance peak in the high-frequency range. For AlAs and AlSb, there are some sharp structures in the low-frequency range and resonance peaks at 4.8 and 3.6 eV, respectively. We find no other theoretical calculation of $\chi^{(3)}(0)$ or $\chi^{(3)}(\omega)$ for the Al compounds.

Figures 7, 8, and 9 show the calculated $\chi_{1111}^{(3)}(\omega)$ and $\chi_{1212}^{(3)}(\omega)$ for GaP, GaAs, and GaSb, respectively. For GaP, $|\chi^{(3)}(\omega)|$ shows two prominent peaks at 1.1 and 1.7

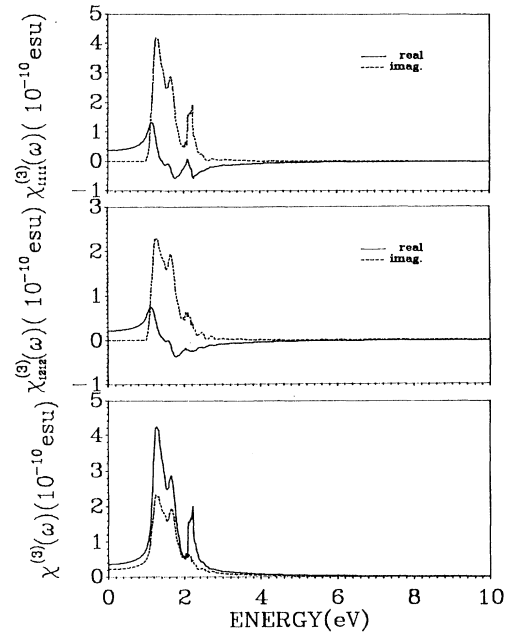


FIG. 2. Calculated third-harmonic generations for Si. Description is the same as Fig. 1.

eV and resonance structures near 3.5 eV. For GaAs, the major structures are at 0.5, 0.9, and 1.6 eV. Our results for GaAs are in reasonable agreement with the calculation of MGSV using the empirical-tight-binding method, which also shows a three-peak structure at approximately the same locations. However, the relative strengths of

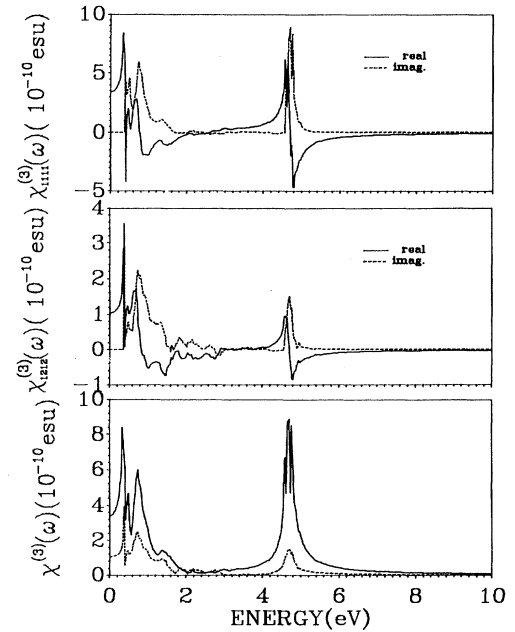


FIG. 3. Calculated third-harmonic generations for Ge. Description is the same as Fig. 1.

TABLE IV. Calculated peak positions in $\chi_{\text{III}}^{(3)}(\omega)$ (in units of eV).

| Crystal | Major peaks | Resonance peak |
|---------|----------------|----------------|
| C | 2.4, 4.4 | |
| Si | 1.3, 1.6, 2.2 | |
| Ge | 0.4, 0.5, 0.7 | 4.7 |
| AlP | 1.3, 1.7, 2.5 | |
| AlAs | 1.2, 1.6 | 4.8 |
| AlSb | 0.8, 1.2, 1.9 | 3.6 |
| GaP | 1.1, 1.7 | 3.5 |
| GaAs | 0.5, 0.9, 1.6 | 6.0 |
| GaSb | 0.27, 0.4, 0.6 | |
| InP | 0.4, 1.0, 2.3 | 4.4 |
| InAs | 0.15, 0.26 | |
| InSb | 0.08 | |
| ZnS | 1.3, 1.8, 2.4 | 3.2 |
| ZnSe | 0.9, 1.6, 2.3 | 4.4 |
| ZnTe | 1.1, 1.7 | 3.3 |
| CdS | 0.9, 1.6, 2.2 | 3.9 |
| CdSe | 0.6, 1.3, 2.6 | 3.8 |
| CdTe | 0.5, 0.9, 2.6 | |

the peaks are not the same. Our calculation also shows a strong resonance peak in the 6.0-eV region in GaAs. For GaSb, low-energy structures at 0.27, 0.37, and 0.57 are well resolved and there is no resonance peak at higher frequencies.

The dispersion relations for $\chi^{(3)}(\omega)$ for InP, InAs, and InSb are shown in Figs. 10, 11, and 12, respectively. For InP, there are many structures in the $|\chi^{(3)}(\omega)|$ spectrum with major peaks at 0.4, 1.0, and 2.3 eV and additional

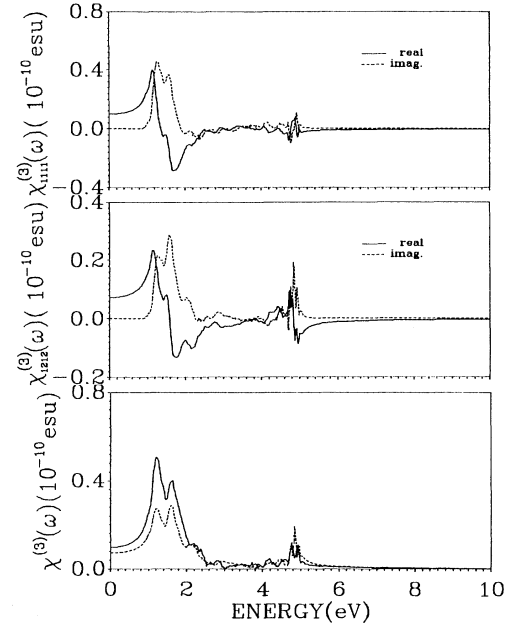


FIG. 5. Calculated third-harmonic generations for AlAs. Description is the same as Fig. 1.

resonance peaks above 4.0 eV. The most prominent one is at 4.4 eV. In contrast to InP, the $|\chi^{(3)}(\omega)|$ spectra for InAs and InSb are very simple, consisting of a single sharp peak at 0.15 and 0.08 eV, respectively. This is consistent with the huge $|\chi^{(3)}(0)|$ values for these two crystals discussed earlier, and is the consequence of their

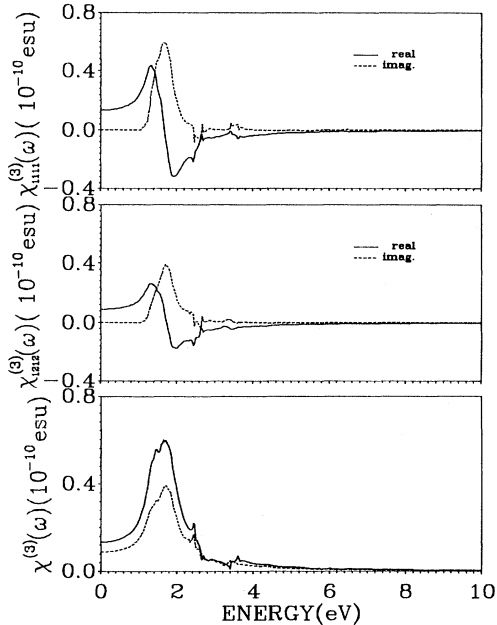


FIG. 4. Calculated third-harmonic generations for AlP. Description is the same as Fig. 1.

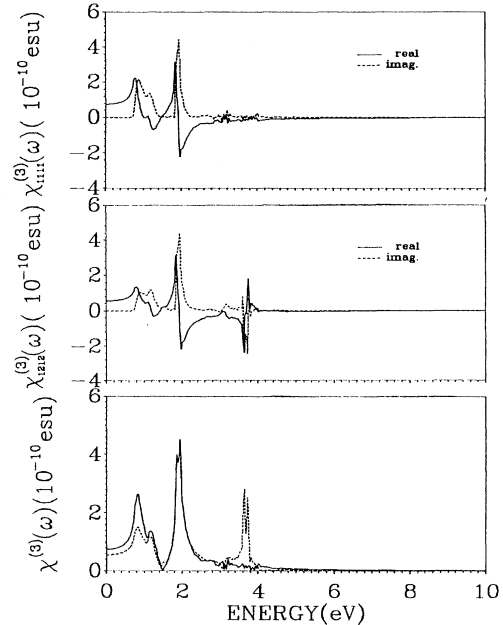


FIG. 6. Calculated third-harmonic generations for AlSb. Description is the same as Fig. 1.

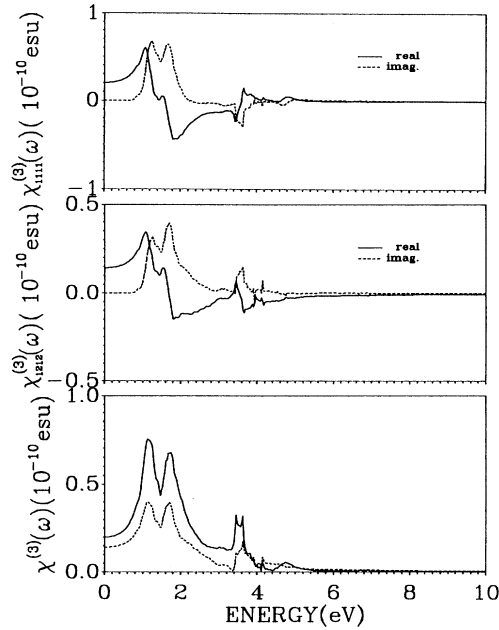


FIG. 7. Calculated third-harmonic generations for GaP. Description is the same as Fig. 1.

small direct gaps at Γ . The presence of additional peaks or resonance structures in these two crystals cannot be ruled out, but are most likely to be of negligible amplitudes in comparison with the major peak. We find no other calculations or measurements of the dispersion relations for the In compounds. The strong single-peak structures for InAs and InSb predicted by our calculation

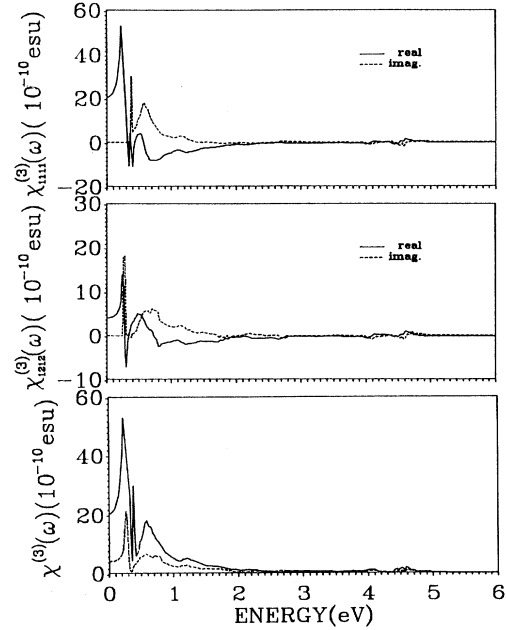


FIG. 9. Calculated third-harmonic generations for GaSb. Description is the same as Fig. 1.

should be easy to detect. The major peak and the resonance peak positions for the III-V compounds are listed in Table IV.

C. II-VI semiconductors

The dispersion curves for $\chi_{1111}^{(3)}(\omega)$ and $\chi_{1212}^{(3)}(\omega)$ for ZnS, ZnSe, and ZnTe are shown in Figs. 13, 14, and 15,

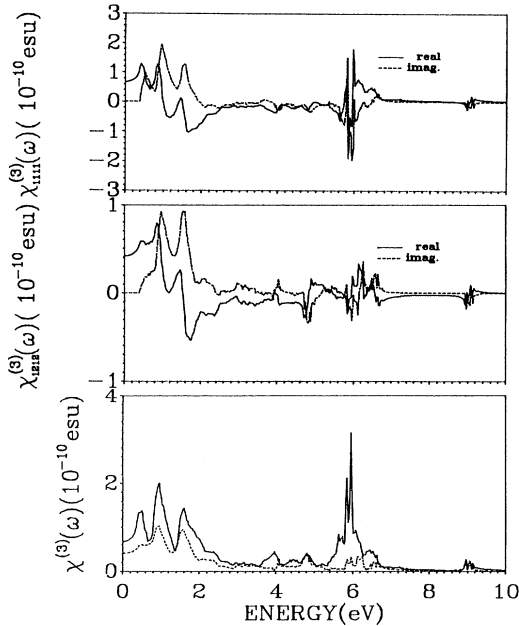


FIG. 8. Calculated third-harmonic generations for GaAs. Description is the same as Fig. 1.

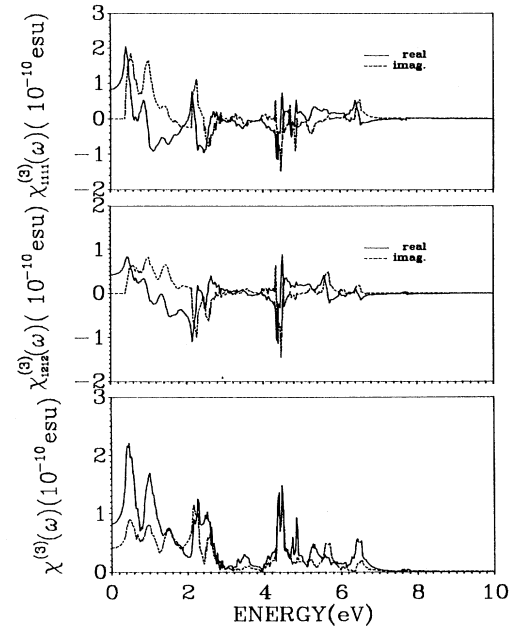


FIG. 10. Calculated third-harmonic generations for InP. Description is the same as Fig. 1.

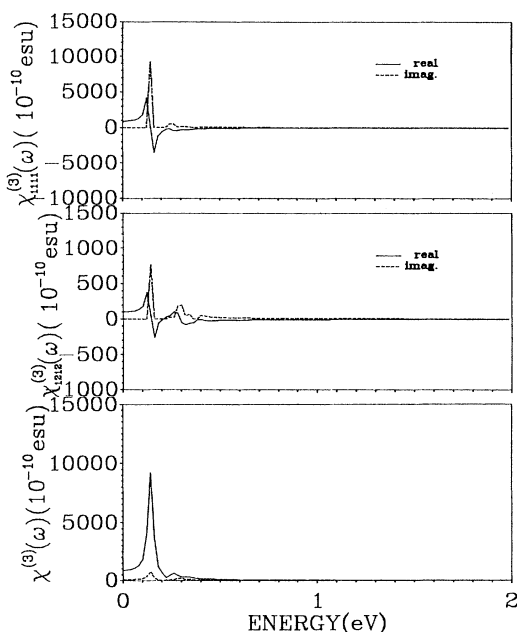


FIG. 11. Calculated third-harmonic generations for InAs. Description is the same as Fig. 1.

respectively, and those of CdS, CdSe, and CdTe are shown in Figs. 16–18. Generally speaking, the dispersion relations for the II–VI compounds are of lower amplitude and the resonance peaks, if they exist, are at lower energies. The general features in $|\chi^{(3)}(\omega)|$ for the II–VI compounds seem to be a three-peak structure in the low-frequency region plus strong resonance peaks at 3.2,

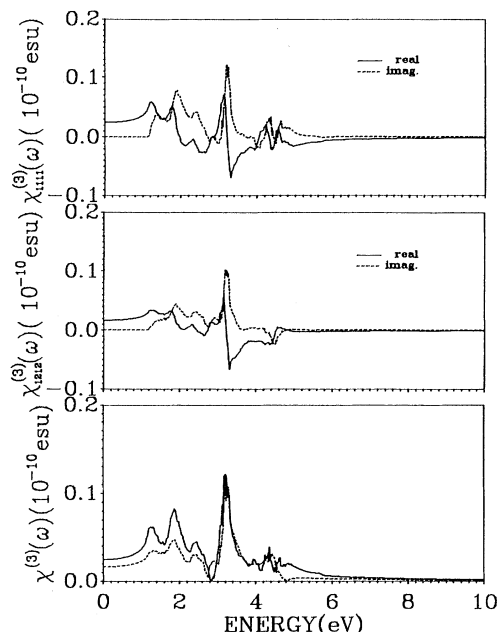


FIG. 13. Calculated third-harmonic generations for ZnS. Description is the same as Fig. 1.

4.4, 3.9, and 2.5 eV for ZnS, ZnSe, CdS, and CdTe, respectively. The major peak positions and the resonance peak positions are listed in Table IV. Again, we find no experimental measurements to compare. GMS have calculated the dispersion curves for the THG in ZnSe, ZnTe, and CdTe.³² Their results for $|\chi^{(3)}(\omega)|$ are in qualitative agreement with ours below the 2.5-eV region ex-

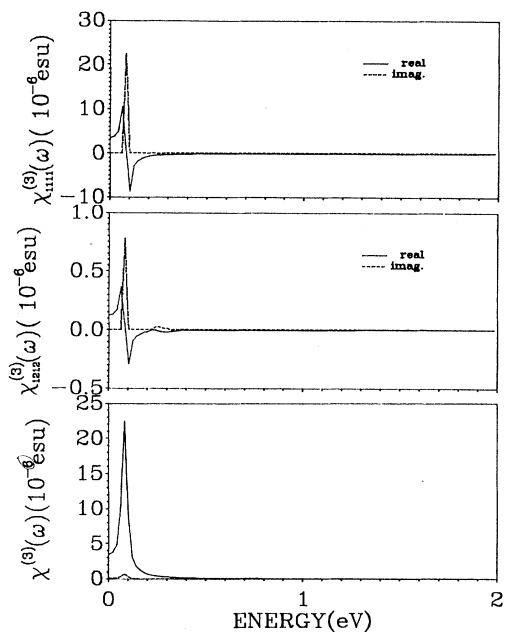


FIG. 12. Calculated third-harmonic generations for InSb. Description is the same as Fig. 1.

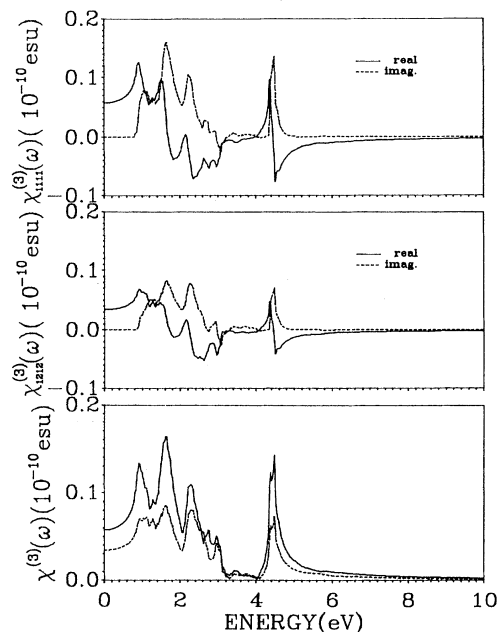


FIG. 14. Calculated third-harmonic generations for ZnSe. Description is the same as Fig. 1.

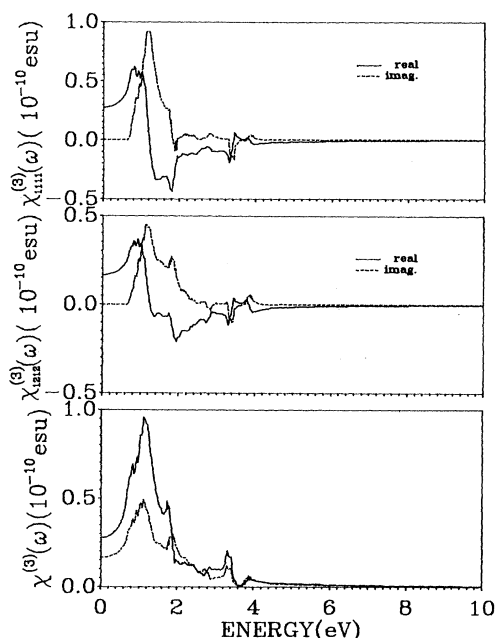


FIG. 15. Calculated third-harmonic generations for ZnTe. Description is the same as Fig. 1.

cept for CdTe, where our calculations show sharp structures at 2.5 eV.

IV. CONCLUSION

With the third-order nonlinear susceptibilities in the form of THG calculated for the 18 semiconductors, it is

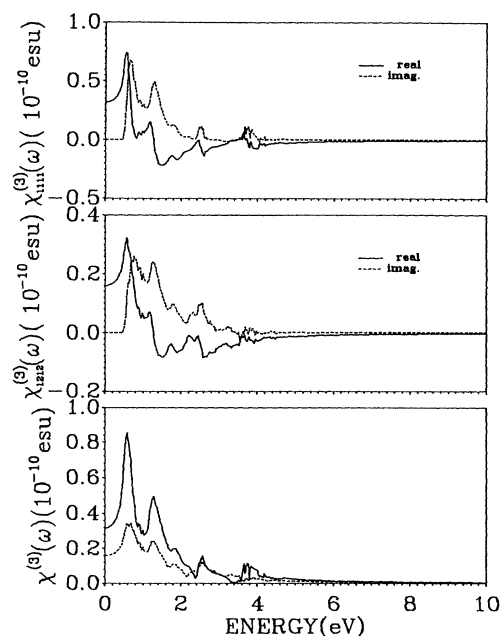


FIG. 17. Calculated third-harmonic generations for CdSe. Description is the same as Fig. 1.

desirable to seek any consistent correlations with other physical parameters. In Fig. 19, we plot the first major peak position in $|\chi_{1111}^{(3)}(\omega)|$ listed in Table IV (multiplied by 3) with the direct band gap. A good linear relationship of unit slope is obtained as expected. In the simplest approximation, the THG involves successive absorptions of three photons of equal frequency. The points off the

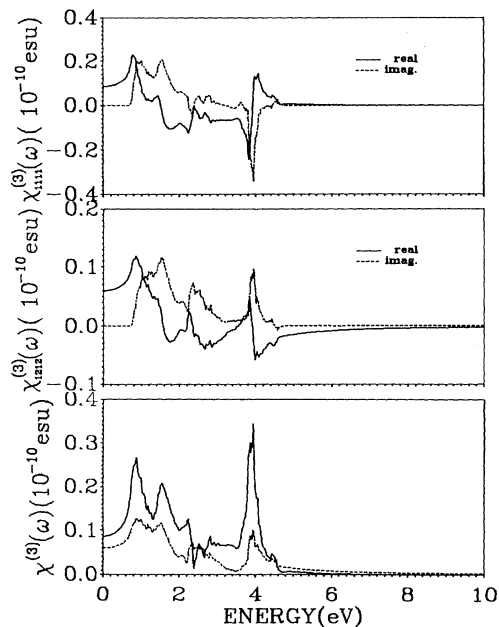


FIG. 16. Calculated third-harmonic generations for CdS. Description is the same as Fig. 1.

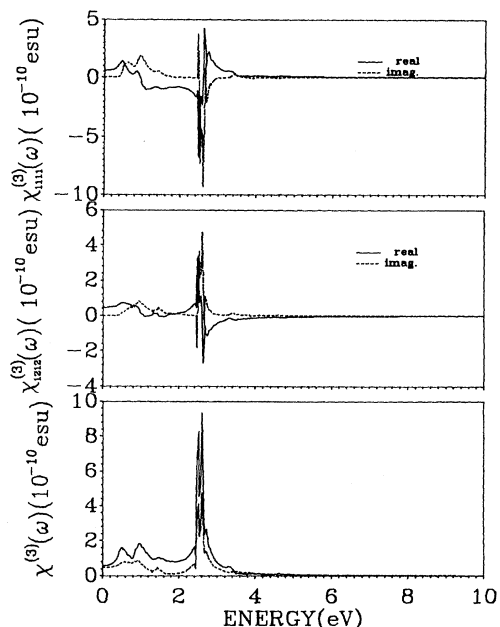


FIG. 18. Calculated third-harmonic generations for CdTe. Description is the same as Fig. 1.

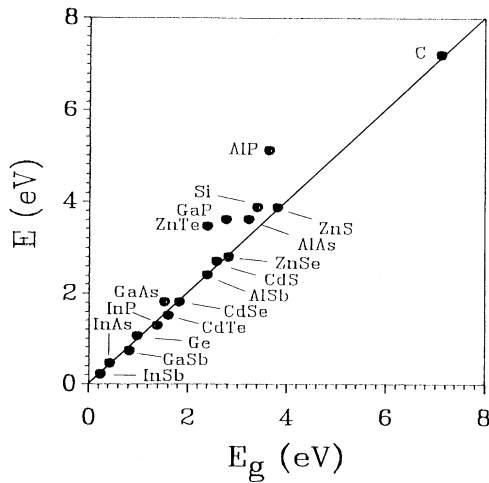


FIG. 19. Correlation between the first major peak in $|\chi_{1111}^{(3)}(\omega)|$ and direct band gap.

line (AlP, GaP, and ZnTe) in Fig. 19 are all above the linear line indicating that in these crystals, the third-order nonlinear process may involve transitions above the minimal direct gap. Such features must be related to the energy bands and the symmetry of the wave functions throughout the entire BZ, and can only be obtained by detailed microscopic calculations.

In Fig. 20, we plot $|\chi_{1111}^{(3)}(0)|$ and $|\chi_{1212}^{(3)}(0)|$ against the direct band gap. As has already been pointed out, the large THG values for some crystals are clearly related to the small band gap. This effect is more accentuated for the THG than for the SHG. In Fig. 21, we plot $|\chi_{1111}^{(3)}(0)|$ and $|\chi_{1212}^{(3)}(0)|$ vs $|\chi_{1111}^{(2)}(0)|$ for those crystals where both elements are nonzero. It is clear that large third-order nonlinearity is always accompanied with a large second-order nonlinearity at least in the cubic semiconductors.

We have presented some detailed theoretical calculations

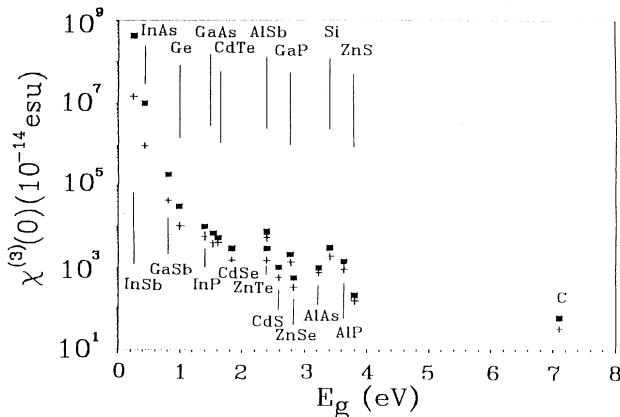


FIG. 20. Correlation between $|\chi_{1111}^{(3)}(0)|$ (■) and $|\chi_{1212}^{(3)}(0)|$ (+) with the direct band gap.

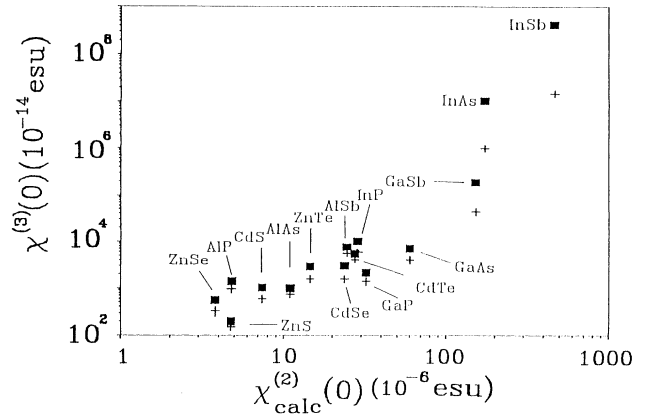


FIG. 21. Correlation between $|\chi_{1111}^{(3)}(0)|$ (■) and $|\chi_{1212}^{(3)}(0)|$ (+) with $|\chi_{1111}^{(2)}(0)|$.

tions on the THG in cubic semiconductors based on the full-band-structure approach using the state-of-the-art local-density calculations. The results show marked improvement over the existing calculations. This is attributed to two factors. First, the full-band-structure approach is a more fundamental and rigorous approach for calculation of nonlinear optical excitations. Second, sufficient numbers of accurately determined CB band states have been included in the sum to ensure proper convergence. Without either of these, it would be very difficult to obtain reliable results consistent with experimental data. The detailed dispersion relations for frequencies up to 10 eV are also investigated. So far, there are no experimental data on the dispersion relations for comparison and our results can be considered theoretical predictions. More accurate measurements and calculations are clearly called for.

Although our calculation of THG and SGH has neglected corrections due for many-particle interactions, and a gap correction procedure in the form of a "scissor operator" is used, we believe these corrections in bulk semiconductors are much less important than the need for accurate electronic structure within the one-electron formalism. Further refinement of calculation beyond the present one-electron level may lead to even better agreement with experiment. The present calculation also shows the effectiveness and the versatility of applying the OLCAO band method for higher-order nonlinear optical calculations. We intend to use the same method to study the nonlinear excitations in other more complicated yet technologically more important materials, and to study high-order nonlinear processes other than harmonic generations.

ACKNOWLEDGMENTS

This work was supported by the Office of Naval Research through Grant No. N00014-91-J-1110. One of us (W.Y.C.) would like to thank Professor John Sipe, Dr. D. Moss, and Dr. Ed. Ghahramani for valuable discussions.

- ¹M.-Z. Huang and W. Y. Ching, paper I, Phys. Rev. B **47**, 9449 (1993).
- ²M.-Z. Huang and W. Y. Ching, paper II, Phys. Rev. B **47**, 9464 (1993).
- ³D. S. Chemla, Rep. Prog. Phys. **43**, 1191 (1980).
- ⁴Y. R. Shen, *The Principles of Nonlinear Optics* (Wiley-Interscience, New York, 1984).
- ⁵S. Singh, in *Handbook of Laser Science and Technology*, edited by M. J. Weber (CRC, Cleveland, 1986), Vol. III, Pt. 1, p. 88.
- ⁶P. N. Butcher and D. Cotter, *The Elements of Nonlinear Optics* (Cambridge University Press, New York, 1990).
- ⁷R. W. Boyd, *Nonlinear Optics* (Academic, New York, 1992).
- ⁸B. S. Wherrett, Proc. R. Soc. London Ser. A **390**, 373 (1983).
- ⁹G. D. Mahan and K. R. Subbaswamy, *Local Density Theory of Polarizability* (Plenum, New York, 1990). This book contains recent references on the calculation of nonlinear optical properties of many ionic crystals.
- ¹⁰W. L. Smith, J. H. Bechtel, and N. Bloembergen, Phys. Rev. B **12**, 706 (1975).
- ¹¹K. R. Subbaswamy and G. D. Mahan, J. Chem. Phys. **84**, 3317 (1986).
- ¹²M. D. Johnson, K. R. Subbaswamy, and G. Senatore, Phys. Rev. B **36**, 9202 (1987).
- ¹³R. Adair, L. L. Chase, and S. A. Payne, Phys. Rev. B **39**, 3337 (1989).
- ¹⁴M. E. Lines, Phys. Rev. B **41**, 3372 (1990); **41**, 3383 (1990); **43**, 11 978 (1991).
- ¹⁵D. F. Eaton, Science **253**, 281 (1991).
- ¹⁶A. Miller, D. A. B. Miller, and S. D. Smith, Adv. Phys. **3**, 697 (1981).
- ¹⁷Y. C. Cheng, J. Appl. Phys. **58**, 499 (1985).
- ¹⁸J. Khurgin, Appl. Phys. Lett. **51**, 2100 (1987).
- ¹⁹I. M. Morrison, M. Jaros, and A. W. Beavis, Appl. Phys. Lett. **55**, 1609 (1989).
- ²⁰I. M. Morrison and M. Jaros, Phys. Rev. B **42**, 3749 (1990).
- ²¹Y. L. Xie *et al.*, Phys. Rev. B **43**, 12 477 (1991).
- ²²S. S. Jha and N. Bloembergen, Phys. Rev. **171**, 891 (1968).
- ²³S. S. Jha and N. Bloembergen, IEEE J. Quantum Electron. **QE-4**, 670 (1968).
- ²⁴B. F. Levine, Phys. Rev. Lett. **22**, 787 (1969).
- ²⁵J. A. Van Vechten, M. Cardona, D. E. Aspnes, and R. M. Martin, in *Proceedings of the Tenth International Conference on the Physics of Semiconductors, Cambridge, MA, 1970*, edited by S. P. Keller, J. C. Hensel, and F. Stern (USAEC Division of Technical Information Extension, Oak Ridge, TN, 1970), p. 82.
- ²⁶C. Flytzanis, Phys. Lett. A **31**, 273 (1970).
- ²⁷C. C. Wang, Phys. Rev. B **2**, 2045 (1970).
- ²⁸D. S. Chemla, R. F. Begley, and R. L. Byer, IEEE J. Quantum Electron. **QE-10**, 71 (1974).
- ²⁹K. Arya and S. S. Jha, Phys. Rev. B **20**, 1611 (1979).
- ³⁰D. J. Moss, J. E. Sipe, and H. M. van Driel, Phys. Rev. B **36**, 9708 (1987).
- ³¹D. J. Moss, E. Ghahramani, J. E. Sipe, and H. M. van Driel, Phys. Rev. B **41**, 1542 (1990).
- ³²E. Ghahramani, D. J. Moss, and J. E. Sipe, Phys. Rev. B **43**, 9700 (1991); **43**, 8990 (1991).
- ³³D. J. Moss, E. Ghahramani, J. E. Sipe, and H. M. van Driel, Phys. Rev. B **34**, 8758 (1986).
- ³⁴M.-Z. Huang and W. Y. Ching, J. Phys. Chem. Solids **46**, 977 (1985).
- ³⁵J. J. Wynne, Phys. Rev. **178**, 1295 (1969).
- ³⁶W. K. Burns and N. Bloembergen, Phys. Rev. B **4**, 3437 (1971).
- ³⁷N. Bloembergen, W. K. Burns, and M. Matsuoka, Opt. Commun. **1**, 195 (1969).
- ³⁸E. Yablonovitch, C. Flytzanis, and N. Bloembergen, Phys. Rev. Lett. **29**, 865 (1972).
- ³⁹M. D. Levenson and N. Bloembergen, Phys. Rev. B **10**, 4447 (1974).
- ⁴⁰D. Weaire, B. S. Wherrett, D. A. B. Miller, and S. D. Smith, Opt. Lett. **4**, 331 (1979).
- ⁴¹D. E. Watkins, C. R. Phipps, and S. J. Thomas, Opt. Lett. **5**, 248 (1980).
- ⁴²D. Depatie and D. Hauelsen, Opt. Lett. **5**, 252 (1980).
- ⁴³D. A. B. Miller, C. T. Seaton, M. E. Prise, and S. D. Smith, Phys. Rev. Lett. **47**, 197 (1981).
- ⁴⁴S. Y. Yuen and P. A. Wolff, Appl. Phys. Lett. **40**, 457 (1982).
- ⁴⁵L. T. Cheng, N. Herron, and Y. Wang, J. Appl. Phys. **66**, 3417 (1989).